Journal of Materials Chemistry C

ROYAL SOCIETY OF CHEMISTRY

PAPER

View Article Online
View Journal | View Issue

Cite this: J. Mater. Chem. C, 2023, 11, 2574

Color-tuning and boosting circularly polarized luminescence performance of axially chiral tetra-BF_2 complexes by post-modifications†

Luxia Cui, [a] Koichi Deyama,[a] Takafumi Ichiki,[a] Yuto Konishi,[a] Ami Horioka,[a] Takunori Harada, [b] Kohei Ishibashi,[b] Yoshio Hisaeda [ac] and Toshikazu Ono *[ac]

The design and synthesis of novel circularly polarized luminescence (CPL) molecular emitters exhibiting photophysical modulation and high CPL efficiency have become an attractive research topic in synthetic and materials chemistry. In this study, three novel axially chiral tetra-BF_2 complexes were rationally designed and synthesized with an easy synthetic approach. The novel terthiophene-substituted tetra-BF_2 complexes were successfully prepared by the Suzuki–Miyaura coupling reaction with an isolated yield of 50% using Br-modified precursors. The terthiophene modification affected absorption, fluorescence, and CPL performance by extending the π-conjugation and improving intramolecular charge transfer (ICT) interactions. One compound, terthiophene modified in the *meta*-position relative to the pyridine moiety of a non-functionalized tetra-BF_2 complex, exhibited a yellow-green emission, whereas another compound, terthiophene modified in the *para*-position, exhibited a yellow emission with a maximum bathochromic shift in both the absorption and emission bands. This is significantly different from unsubstituted and Br-modified compounds, which fluoresced in the green region by the π–π* transition. Moreover, the compound, in which the *para*-position to the pyridine part in the framework of the tetra-BF_2 complex was substituted by terthiophene moieties, exhibited excellent CPL performance with a high dissymmetric factor (g_{lum} up to the order of 10^{-2}) and CPL brightness (B_{CPL}) at 125.2 M^{-1} cm^{-1} in toluene owing to the balance of electric and magnetic transition dipole moments compared with those of other tetra-BF_2 complexes. This work opens a new avenue for developing novel organic CPL emitters by inducing ICT characters to modulate the emission color and high CPL efficiency.

Received 1st November 2022,
Accepted 10th January 2023

DOI: 10.1039/d2tc04636a

rsc.li/materials-c

Introduction

Advancing the construction of novel chiral systems exhibiting circularly polarized luminescence (CPL) has attracted increasingly significant attention from researchers owing to their widespread application in chemical sensors, biological probes, organic optoelectronic devices, and security inks.[1–6] Generally, simple CPL-active organic molecules include those based on helicene,[7–12] helical structures,[13–15] binaphthyl,[16–19] cyclophane,[20–23] chiral macrocycles,[24,25] molecular assemblies,[26–31] and coordination-based complexes.[6] This is attributed to their definite and diverse structures with good solubility and availability to modify the structures by replacing various substituents. Typically, moderate CPL performance is frequently observed in solutions for these purely organic molecules with a luminescence dissymmetry factor (g_{lum}) in the range of 10^{-5}–10^{-3} as well as tedious synthesis processes, far away from the practical requirements.[32,33] Therefore, it remains a significant challenge to achieve a high g_{lum} value with tunable photophysical properties by the rational design of molecular engineering.

In the past decades, organoboron complexes (typically, BODIPY) have piqued significant interest because of their structural versatility and excellent photophysical properties in the applications of chemosensors, biological imaging and labeling, photodynamic therapy, and optoelectronic devices.[34–36] However, the development of CPL-active organoboron chiral systems is hindered because most organoboron complexes have planar and achiral structures.[6,37] Constructing chiral organoboron complexes with CPL properties is achievable by incorporating

[a] Department of Chemistry and Biochemistry, Graduate School of Engineering, Kyushu University 744 Motooka, Nishi-ku, Fukuoka, 819-0395, Japan. E-mail: tono@mail.cstm.kyushu-u.ac.jp
[b] Faculty of Science and Technology, Graduate School of Engineering, Oita University 700 Dannoharu, Oita City, 870-1192, Japan
[c] Center for Molecular Systems (CMS), Kyushu University 744 Motooka, Nishi-ku, Fukuoka, 819-0395, Japan

† Electronic supplementary information (ESI) available. See DOI: https://doi.org/10.1039/d2tc04636a

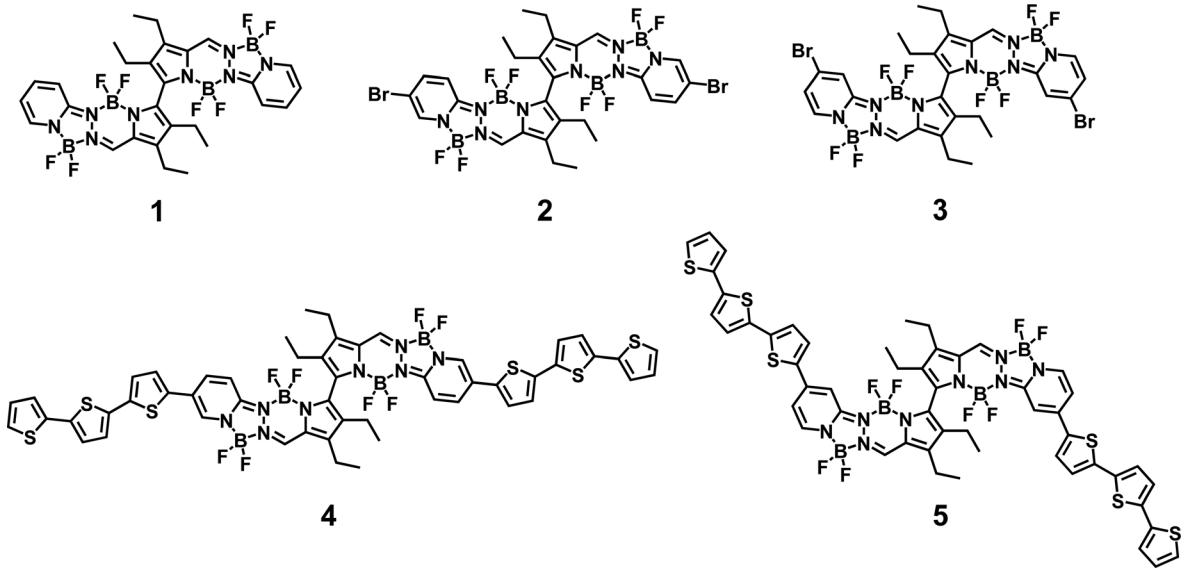

Fig. 1 Chemical structures of compounds **1–5**.

chiral perturbation into organoboron complexes. Thus far, a considerable number of optically active BODIPYs have been investigated by incorporating chiral substituents with tetra-boron difluoride (BF_2)-configurations, a boron-bridged orthogonal combination fluorophore and chiral elements, or those with boron as a chiral center attributed to tetra-coordination induced asymmetry.[6,37,38] However, achieving diverse chiral organoboron complexes based on other BODIPY congeners such as BOPHY,[39–41] BOPPY,[42] and BOPAHY[43–45] remains challenging. In 2022, our group demonstrated a series of novel tetra-BF_2 complexes with multicolor photoluminescence in a green-to-orange region in solutions, high quantum yields (up to 100%), and large Stokes shifts. Axial chirality introduced by a steric hindrance from tetra-ethyl substituents on the 2,2′-bipyrrole moiety in tetra-BF_2 complexes achieved efficient CPL performance (Fig. 1, compounds **1** and **2**).[46] These novel CPL-active tetra-BF_2 complexes suffer from the limited green emission color in solutions and a common g_{lum} value (in the order of 10^{-3}) even though they exhibited high quantum yields of up to *ca.* 60%. Therefore, it is highly desirable to develop a new molecular structure to achieve tunable emission color and improve the CPL performance with a higher g_{lum} value to meet the increasing requirements of CPL-responsive systems.

For a chiral system, typically, the dissymmetry factor (g_{abs} or g_{lum}) illustrated the difference between the left-handed and right-handed circularly polarized (CP) light in absorption or emission, expressed as $g = 2(I_L - I_R)/(I_L + I_R)$, where I_L and I_R represent the intensities of left- and right-handed circularly polarized light in absorption or emission. The g-value in an electronic transition between i and j states is a function of the rotational strength R_{ij} and the dipole strength D_{ij} [eqn (1)]:

$$g = \frac{4R_{ij}}{D_{ij}} = \frac{4|\mu_{ij}||m_{ij}|\cos\theta_{ij}}{|\mu_{ij}|^2 + |m_{ij}|^2} \quad (1)$$

where μ_{ij} and m_{ij} represent the electric and magnetic transition dipole vectors, respectively, and θ_{ij} represents the angle between them. For most single organic molecules, $|\mu_{ij}| \gg |m_{ij}|$, and [eqn (1)] can be approximated as [eqn (2)]:

$$g = \frac{4|m_{ij}|\cos\theta_{ij}}{|\mu_{ij}|} \quad (2)$$

Thus, the dissymmetry factor (g_{abs} and g_{lum}) is dominated by the transition dipole moments of its electronic transition. The dissymmetry factor of CP light in emission, g_{lum}, reflects the structure in the excited state, whereas the structure in the ground state assesses g_{abs}. The g-value enhancement is achievable by suppressing μ_{ij}, extending m_{ij}, and increasing the value of $\cos\theta$.[25] Recently, high g_{lum} values reaching higher than 10^{-3} order for small organic molecules were achieved by some chiral systems based on heliene and perylene diimide by the modulation of the magnitude and relative orientation of the μ and m vectors.[9,24,47,48] For example, K. Matsuda and co-workers reported that introducing substitution in the [7]helicene framework can achieve a large m for the $S_1 \rightarrow S_0$ transition to yield a high g_{lum} of up to 1.3×10^{-2} in the solution state.[9] W. Jiang *et al.* presented a double-helical π-conjugated system based on a cyclooctatetraene-embedded perylene diimide dimer exhibiting a maximal g_{lum} of 0.03 resulting from the slight decreases of μ and significant increases of m, thus boosting the CPL performance remarkably.[47] However, g_{lum} is insufficient as it considered only the relative imbalance of CP light in emission. In 2021, Francesco Zinna and colleagues proposed calculating CPL brightness (B_{CPL}) [eqn (3)] to assess the overall merit of a CPL emitter.[49]

$$B_{CPL} = \varepsilon_\lambda \times \phi \times \frac{|g_{lum}|}{2} \quad (3)$$

where ε_λ represents the molar extinction coefficient measured at the excitation wavelength (λ), and φ represents the emission quantum yield. In this case, balancing the ε_λ, φ, and g_{lum} to

achieve intense B_{CPL} is in high demand to satisfy the development of globally more performant CPL emitters.

To achieve this goal, herein, rationally designed terthiophene-modified tetra-BF_2 complexes (**4** and **5**) were first synthesized by the Suzuki–Miyaura coupling reaction using **2** and **3** as precursors, respectively (Fig. 1 and Scheme 1). The experimental data and theoretical calculations suggested that introducing terthiophene moieties on tetra-BF_2 complexes extended the π-conjugation effect and endowed a strengthened intramolecular charge transfer (ICT) character compared with the non-functionalized tetra-BF_2 complex **1**. The substituted position of terthiophene moieties makes a difference in the photophysical properties to provide a yellow-green emission in **4** and yellow emission in **5**, whereas compounds **1–3** exhibited a limited green emission color. Furthermore, compound **5** exhibited a significantly enhanced CPL response with a high g_{lum} of up to the order of 10^{-2} and excellent B_{CPL} (125.2 M^{-1} cm^{-1}) even though compounds **1–4** yielded a typical 10^{-3} order of g_{lum}. To the best of our knowledge, this is the first report on the rational molecular engineering of tetra-BF_2 complexes for color-tuning and improving the CPL performance.

Results and discussion

Compounds **1** and **2** were prepared according to the established methods.[46] Compound **3** was newly synthesized using tetra-ethyl modified 5,5′-diformyl-2,2′-bipyrrole and 4-bromo-2-hydrazinopyridine as reactants, where 4-bromo-2-hydrazinopyridine was obtained by reacting 4-bromo-2-fluoropyridine with hydrazine monohydrate in ethanol (Scheme S1 and Fig. S1, ESI†). The Suzuki–Miyaura coupling reactions in **2** or **3** and an excess of 2,2′:5′,2″-terthiophene-5-boronic acid pinacol ester at 90 °C in a 1,4-dioxane/H_2O mixture afforded the corresponding terthiophene-substituted **4** and **5** both in 50% yields (Scheme 1). For more details, see the ESI.† A combination of nuclear magnetic resonance (NMR) spectroscopy (^1H, ^{13}C, ^{19}F, and ^{11}B NMR) and high-resolution mass spectrometry confirmed the formation of the newly desired products **3–5** (Fig. S2–S4, ESI†).

The ultraviolet-visible (UV-vis) absorption and fluorescence spectra of **1–5** have been fully investigated in solutions, and the corresponding optical data are summarized in Fig. 2 and Fig. S5–S10 (ESI†), and Table 1, Tables S1 and S2 (ESI†). In toluene, compound **1** exhibited absorption maxima at 404 nm and 452 nm, with extinction coefficients of 5.61×10^4 and 7.14×10^4 M^{-1} cm^{-1}, respectively. The red-shifted absorption bands were observed at 440 nm (1.58×10^4 M^{-1} cm^{-1}) and 486 nm (4.79×10^4 M^{-1} cm^{-1}) for **4**, and a broad absorption band with a maximum at 436 nm (6.95×10^4 M^{-1} cm^{-1}) for **5** (Fig. 2a and Table 1). Compounds **4** and **5** both exhibited a bathochromic shift in emission spectra compared with compounds **1–3**. Among them, compound **5** exhibited the longest emission maximum (λ_{em}^{max}) at 550 nm and a Stokes shift to 4800 cm^{-1}, whereas the λ_{em}^{max} of **1** was at 514 nm with a Stokes shift to 2700 cm^{-1}, and that of **4** shifted to 534 nm with a Stokes shift at 1900 cm^{-1} (Fig. 2b and c, and Table 1). These findings suggested that (i) the red-shifted emission band in **4** and **5** demonstrated more improved ICT interactions resulting from the terthiophene modification than that in **1**; (ii) the different substituent positions of the terthiophene group in **4** and **5** tuned π-conjugation extension and the highest occupied molecular orbital (HOMO)–lowest unoccupied molecular orbital (LUMO) gap to achieve different photophysical properties. Compounds **4** and **5** both produced high photoluminescence quantum yields of 54% and 36%, respectively, with a lifetime of 1.57 ns for **4** and 1.70 ns for **5** (Table 1). To understand the electronic properties of these tetra-BF_2 complexes, their ground state geometries were optimized by density functional theory (DFT) calculations using the B3LYP/6-31G(d,p) level (Fig. 2d and Fig. S18, ESI†). For compound **4**, the HOMO electronic distributions are delocalized over the whole molecule, and the

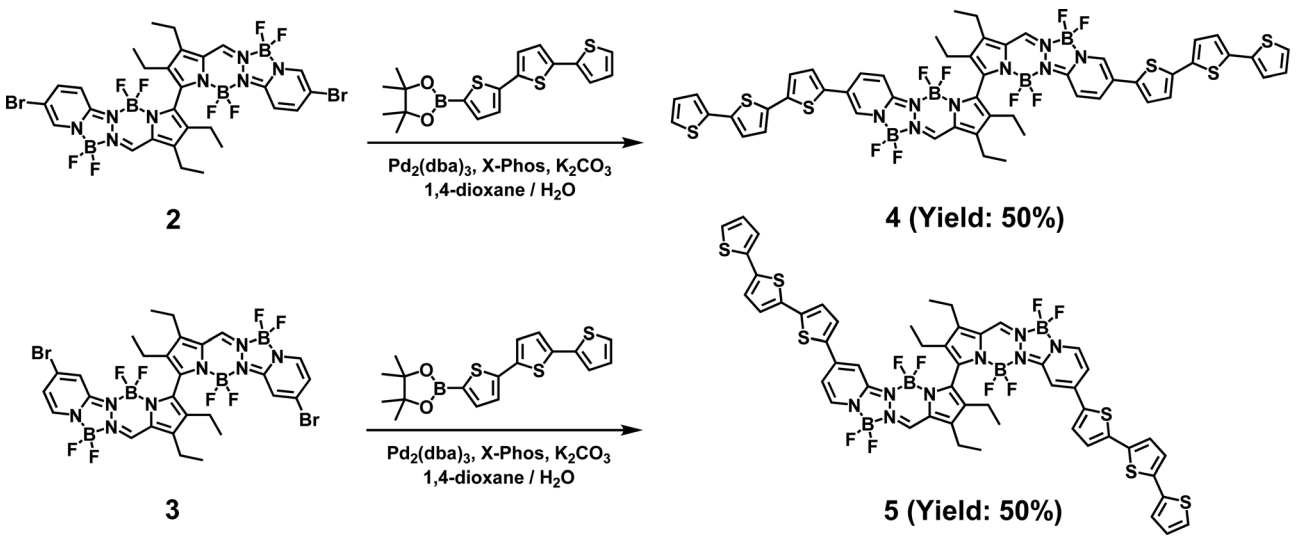

Scheme 1 Synthesis of compounds **4** and **5** by the Suzuki–Miyaura coupling reaction.

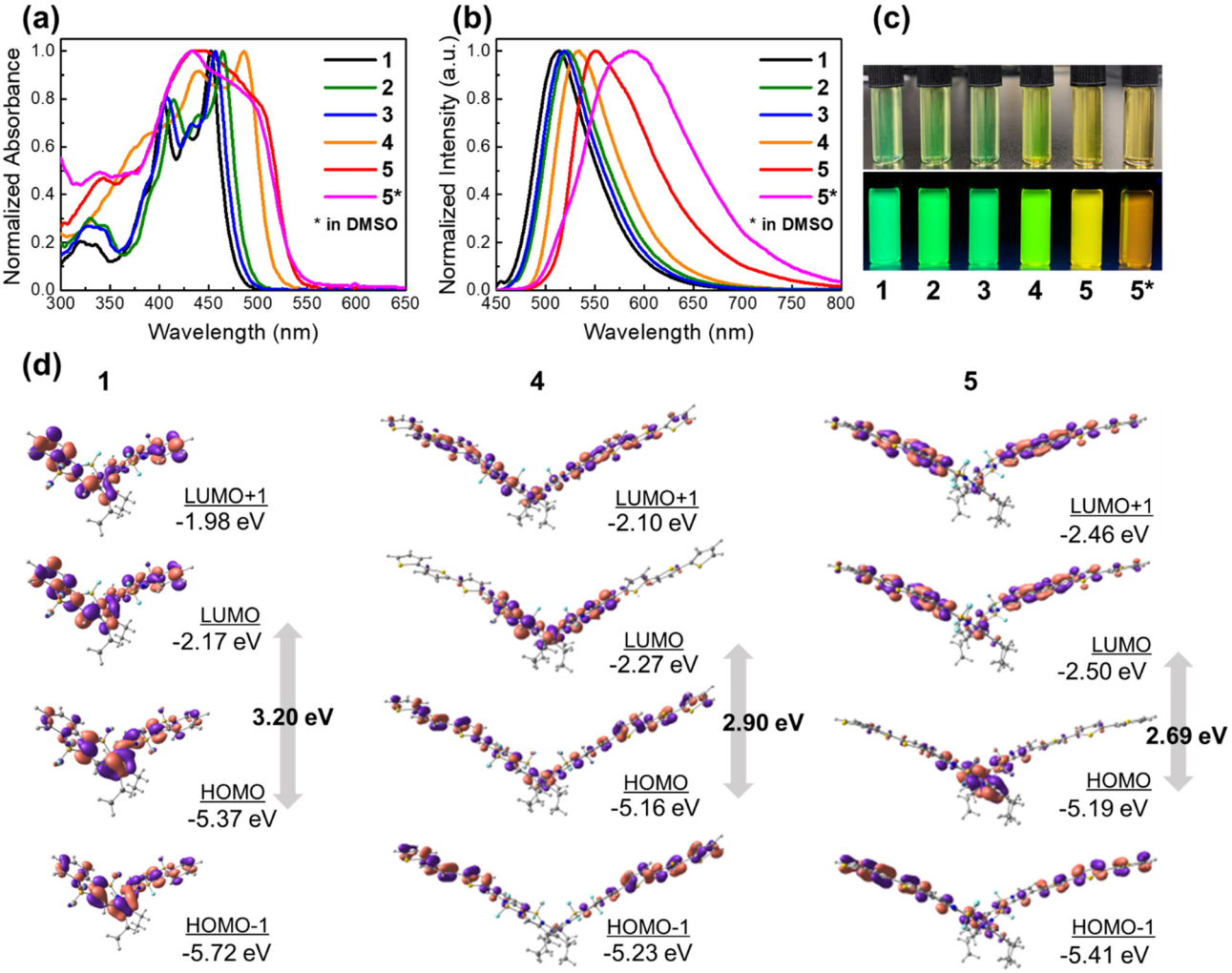

Fig. 2 Normalized (a) UV-vis absorption and (b) emission spectra of **1–5** in toluene with **5** in DMSO (10^{-6} M), excited at λ_{abs}^{max}. (c) Photographs of **1–5** in toluene with **5** in DMSO under daylight (upper row) and 365 nm UV-light irradiation (bottom row). (d) Frontier molecular orbitals of **(*S*)-1**, **(*S*)-4**, and **(*S*)-5**.

Table 1 Photophysical properties of **1–5** in toluene

Compd.	$\lambda_{abs}^{max\,a}$ (nm)	$\lambda_{em}^{max\,b}$ (nm)	$\Phi_{PL}{}^{c}$	τ_{av} (ns)	Stokes shift (cm^{-1})
1	404, 452	514	0.58	2.06	2700
2	414, 464	522	0.58	2.15	2400
3	408, 457	519	0.54	1.76	2600
4	440, 486	534	0.54	1.57	1900
5	436	550	0.36	1.70	4800
5^{d}	432	585	0.13	0.57	6100

^{a} Absorption maxima in toluene ($c = 10^{-6}$ M). ^{b} Emission maxima in toluene, excited at λ_{abs}^{max}. ^{c} Absolute photoluminescence quantum yields, excited at λ_{abs}^{max}. ^{d} In DMSO.

LUMO is primarily localized in other parts, except for terthiophene moieties. For compound **5**, the HOMO is mainly localized at the bipyrrole part, and the electron density of the LUMO is distributed at moieties between the bipyrrole and terthiophene groups, indicating an ICT feature. In contrast, the HOMO and LUMO of compound **1** are both localized over the whole molecule, suggesting a π–π* transition rather than ICT interactions. DFT calculations elucidated that the substituted position of terthiophene on the tetra-BF_2 complexes resulted in the almost opposite electronic contributions of the HOMO and LUMO for compounds **4** and **5**, respectively, affecting the π-conjugation and ICT interactions. The calculated HOMO–LUMO energy gaps were 3.20, 2.90, and 2.69 eV for **1**, **4**, and **5**, respectively. Time-dependent DFT (TD-DFT) calculations were performed at the cam-B3LYP/6-31G(d,p) level to assign the nature of the absorptions observed in the UV-vis spectra (Fig. S19–S21 and Table S6, ESI†). The strong absorption bands observed for **1**, **4**, and **5** are mainly attributed to $S_0 \rightarrow S_1$ electronic transitions. The molecular orbital distributions of other related HOMOs and LUMOs of **4** and **5** further illustrate that the abovementioned transitions involve varying degrees of ICT (Fig. 2d). These findings implied that compound **5** exhibited an obviously enhanced ICT character compared to **4**, leading to red-shifted optical properties. Both the π-conjugation extension and enhanced ICT interactions observed in **4** and **5** affected the magnitude and relative orientation of μ and m vectors to modulate CPL performance as expected. The DFT-optimized structures of the S_0 and S_1 states of **4** and **5**

revealed that in the S_1 state, the N–C–C–C dihedral angle around the single bond of bipyrrole was smaller than that in the S_0 state, suggesting a more planar conformation due to the structural relaxation (Fig. S22 and S23, ESI†).

To investigate the ICT characters for **4** and **5**, we evaluated the optical properties in various solvents, such as tetrahydrofuran (THF), dichloromethane (DCM), methanol (MeOH), and dimethyl sulfoxide (DMSO), and summarized the optical data in Fig. S5–S10, and Tables S1 and S2 (ESI†). For comparison, the optical properties of compounds **1–3** were also evaluated in these solvents. No obvious solvent-dependent absorption and fluorescence behavior were observed in **1–3**, whereas compounds **4** and **5** exhibited a solvent-dependent emission band with a bathochromic shift accompanied by the decreasing quantum yields with increasing solvent polarity in the order of toluene, THF, DCM, and DMSO. Particularly, the largest λ_{em}^{max} of 585 nm in emission spectra was obtained by compound **5** in DMSO with a Stokes shift at 6100 cm^{-1} (Fig. S7, Table 1 and Table S1, ESI†). These results indicated that the significant ICT feature was due to the introduction of electron-donating terthiophene.

To understand the emission mechanism of **5** in detail, temperature-dependent photoluminescence measurement was performed in 2-methyl-THF (2-MeTHF) (Fig. 3 and Fig. S11, ESI†). As the temperature decreased from 300 K to 77 K at every 30 K cooling rate, the intensity of the emission peak gradually increased with the blue-shifted emission maxima. Note that the emission intensity and wavelength were significantly different from the freezing point of 2-MeTHF (137 K) (Fig. 3a, b, and Fig. S11, ESI†). Reversible behaviors were observed when increasing the temperature in the same way (Fig. 3c, d, and Fig. S11, ESI†). These findings indicated that the large Stokes shift of **5** was attributed to the structural relaxation in the excited state, which was inhibited in the freezing environment.

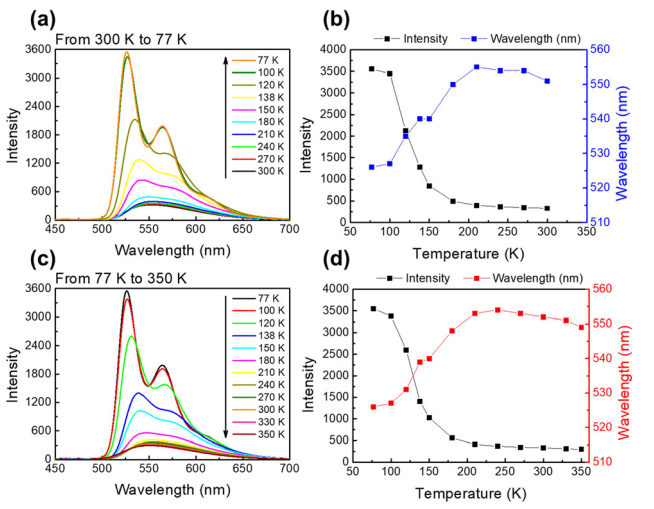

Fig. 3 Optical properties of **5** in 2-MeTHF ($c = 10^{-6}$ M) cooling from 300 K to 77 K (a and b) and heating from 77 K to 350 K (c and d). (a and c) Emission spectra (excited at 430 nm) and (b and d) relationships of emission intensity and wavelength at different temperatures.

Owing to the presence of both axial chirality and photoluminescence, **4** and **5** are expected to exhibit CPL. After the optical resolution by chiral preparative high-performance liquid chromatography (HPLC) (Fig. 4 and Table S3, ESI†), a perfect mirror image symmetry in the circular dichroism (CD) spectra of optically resolved enantiomers **4** and **5** was observed in solutions (Fig. 5a and Fig. S13, ESI†). The absolute configurations of the enantiomers were determined according to the experimental and TD-DFT simulated CD spectra, namely, positive for (***S***)- and negative for (***R***)-enantiomers observed from 600 to 300 nm, respectively (Fig. S19–S21, ESI†). We investigated the CD spectra of compound **5** when adjusting the absorbance at 0.2, 0.5, and 1.2 in toluene (Fig. S12, ESI†), and no concentration dependency was observed.

Upon excitation with UV light, CPL spectra were recorded from 485 to 700 nm. In toluene, strong left- and right-handed CPL signals, namely, positive for the (***S***)-enantiomer and negative for the (***R***)-enantiomer, were observed with a virtual mirror image relationship (Fig. 5b), where the maximum CPL peaks correspond to the photoluminescence emission maxima. Compounds **4** and **5** afford very distinct luminescence dissymmetry factors ($|g_{lum}|$) in toluene. Compound **4** yields a $|g_{lum}|$ value of 0.004, whereas compound **5** produces a higher $|g_{lum}|$ value of 0.01 (Fig. 5b and Table 2). Similar CD and CPL spectra of **5** are also obtained in polar DMSO (Fig. S13, ESI†). In DMSO, compound **5** yields a lower $|g_{lum}|$ value of 0.003, indicating its sensitivity to the polar environment. These results were supported by the TD-DFT calculations (Fig. 5c, Table 2 and Tables S6–S10, ESI†). Firstly, the calculated $|g_{abs}|$ value of 7.60×10^{-3} associated with the $S_0 \rightarrow S_1$ transition of **5** is over one and a half times that of **1** ($|g_{abs}| = 4.74 \times 10^{-3}$), while compound **4** exhibited a $|g_{abs}|$ value of only 2.72×10^{-3} (Tables S6, S8, and S9, ESI†). Hence, **5** is expected to have a large $|g_{lum}|$ value. Indeed, the analysis of the relevant μ and m vectors for the $S_1 \rightarrow S_0$ transitions in **1**, **4**, and **5** was performed (Fig. 5c, Table 2, Tables S7 and S10, ESI†). The calculated angle $\theta_{\mu,m}$ between μ and m is 124.2° for **1**, 108.1° for **4** and 130.7° for **5**, respectively (Table 2). Interestingly, μ is aligned along the pyridine part of tetra-BF_2 complexes and its orientation remains unchanged after the modification of terthiophene moieties, only the magnitude of the μ vector is different (*i.e.* $|\mu| = 1040.50 \times 10^{-20}$ esu cm for **1**; $|\mu| = 1568.54 \times 10^{-20}$ esu cm for **4**; $|\mu| = 1341.40 \times 10^{-20}$ esu cm for **5**), whereas the arrangement of the m vector of **4** and **5** is effectively changed compared to that of **1**. Compounds **4** and **5** both exhibited higher $|m|$ values of

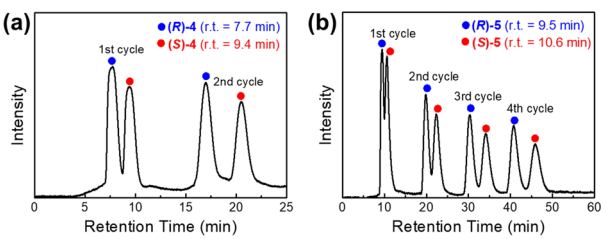

Fig. 4 Chiral HPLC profiles for the separation of enantiomers of **4** and **5**. Fraction 1 (blue) = (***R***)-enantiomer, Fraction 2 (red) = (***S***)-enantiomer.

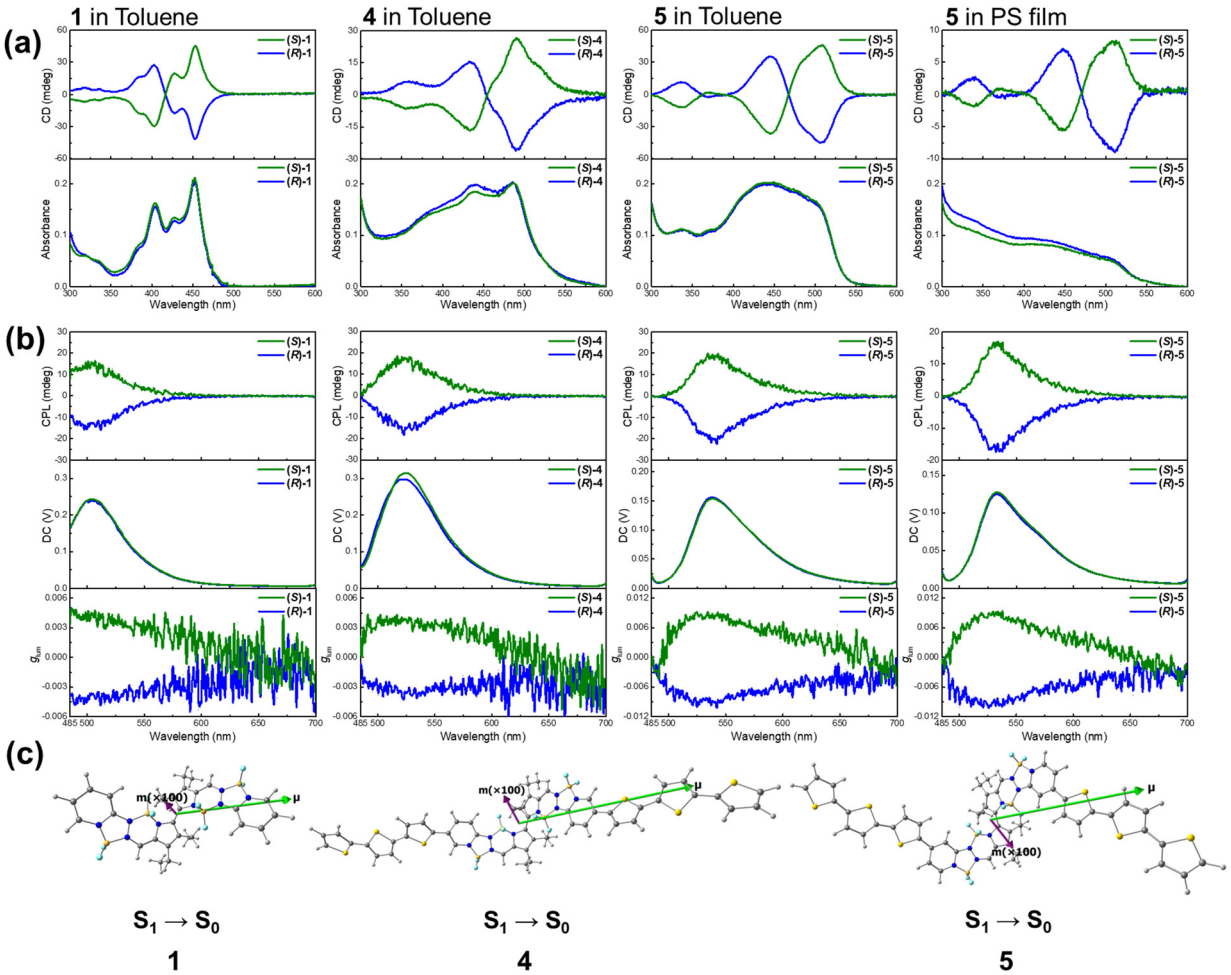

Fig. 5 (a) CD and absorption spectra of **(*R*)-1**, **(*S*)-1**, **(*R*)-4**, **(*S*)-4**, **(*R*)-5**, and **(*S*)-5** in toluene ($c = 10^{-6}$ M), and **(*R*)-5** and **(*S*)-5** in the PS film. (b) CPL, DC (= nonpolarized fluorescence) and g_{lum} spectra of **(*R*)-1**, **(*S*)-1**, **(*R*)-4**, **(*S*)-4**, **(*R*)-5**, and **(*S*)-5** in toluene ($c = 10^{-6}$ M), and **(*R*)-5** and **(*S*)-5** in the PS film. Excited at 415 nm for **1**, and 420 nm for **4** and **5**. (c) Electric (μ, green) and magnetic (m, purple) transition dipole moments associated with the $S_1 \rightarrow S_0$ transition for **1**, **4**, and **5**, where the length of the m vector is multiplied by 100 for clarity.

Table 2 Photophysical parameters and B_{CPL} of compounds **1**, **4**, and **5**

Experimental data in toluene					Calculated data by TD-DFT						
Compd.	ε/M^{-1} cm^{-1} (λ_{abs}^{max}/nm)	Φ_{PL}	$\lvert g_{lum}\rvert$	B_{CPL}/M^{-1} cm^{-1}	Electronic transition	Energy/nm	$\lvert\mu\rvert$/10^{-20} esu cm	$\lvert m\rvert$/10^{-20} erg G^{-1}	θ/°	cos θ	$\lvert g_{lum}\rvert^{cal}$
1	71400 (452)	0.58	0.004	82.88	$S_1 \rightarrow S_0$	450	1040.50	1.33	124.2	−0.56	2.86×10^{-3}
4	47900 (486)	0.54	0.004	51.74	$S_1 \rightarrow S_0$	467	1568.54	3.02	108.1	−0.31	2.39×10^{-3}
5	69500 (436)	0.36	0.01	125.19	$S_1 \rightarrow S_0$	477	1341.40	3.25	130.7	−0.65	6.32×10^{-3}

3.02×10^{-20} erg G^{-1} and 3.25×10^{-20} erg G^{-1}, respectively, while the $|m|$ of **1** is only 1.33×10^{-20} erg G^{-1}. The balance of both the magnitude and relative orientation of the μ and m vectors for the $S_1 \rightarrow S_0$ transitions is the key factor to modulate the $|g_{lum}|$ value. Compound **5** showed a larger $|m|$ value and similar θ to achieve a more than twice $|g_{lum}|$ value ($|g_{lum}| = 6.32 \times 10^{-3}$) than compound **1** ($|g_{lum}| = 2.86 \times 10^{-3}$), whereas **4** displayed a similar $|g_{lum}|$ value of 2.39×10^{-3} which is comparable to **1** owing to the lower $|\cos\theta|$ value despite an extending m. The calculated $|g_{lum}|$ values are well in agreement with the experimental data. This distinctive chiroptical behavior in **5** is attributed to the largely enhanced π-conjugation and ICT interactions by introducing electron-donating terthiophene groups at the *para*-position to the pyridine part in the tetra-BF_2 complexes. Actually, introducing electron donor or acceptor units into a carbo[6]helicene system to optimize the mutual orientation of μ and m in the excited state for strong CPL performance has been developed by L. Favereau and co-workers.[48] This obtained new family of π-helical push–pull carbo[6]helicene-based systems achieved high g_{lum} values reaching 3–4 $\times 10^{-2}$ at the molecular level. However, instead of the widely studied helicene-based chiral system, our work demonstrated the impact of the substitution effect on the chiroptical properties of

organoboron complexes utilizing both experimental and theoretical calculation results, providing a reliable guideline for designing ideal boron-based CPL emitters with a large $|g_{lum}|$ value.

CPL brightness (B_{CPL}) is another important parameter of CPL-active systems.[49] The value of B_{CPL} in toluene is evaluated as 82.9 M^{-1} cm^{-1} for **1**, 51.7 M^{-1} cm^{-1} for **4**, and 125.2 M^{-1} cm^{-1} for **5**, respectively (Table 2). This value is comparable to the reported highest B_{CPL} of the chiral boron complexes.[49]

To evaluate the solid-state chiroptical properties of **5**, the CD and CPL measurements were conducted in KBr disks (Fig. S14, ESI†). The CD signals of **5** enantiomers were obtained with a mirror image; however, CPL response was not achieved. This suggested that the fluorescence emission of **5** was suppressed in the polar environment. Therefore, we prepared the [(***R***/***S***)-**5**]-doped poly(methyl methacrylate) (PMMA) film and polystyrene (PS) film to evaluate the chiroptical properties in the solid states (Fig. 5 and Fig. S14, ESI†). The CD and CPL spectra recorded for [(***R***/***S***)-**5**]-doped PMMA and PS films exhibited mirror image signals of the same handedness as those recorded in solutions (Fig. 5 and Fig. S14, ESI†). The CPL signals of the (***R***)-**5** and (***S***)-**5** enantiomers have opposite signs, which proves the existence of a contribution that corresponds to CPL. The $|g_{lum}|$ values of [**5**]-doped PMMA and PS films were estimated to be between 0.007 and 0.009. The [**5**]-doped PS film exhibited a λ_{em}^{max} of 542 nm, whereas the λ_{em}^{max} of the [**5**]-doped PMMA film was 534 nm (Fig. S15, and Table S4, ESI†). The photoluminescence quantum yield of 43% was achieved by the [**5**]-doped PS film, whereas that of the [**5**]-doped PMMA film is 36%, respectively, with a lifetime of around 2.0 ns (Fig. S16, Tables S4 and S5, ESI†).

In particular, the intensities in the CD spectra of **5** were well preserved, even after 358 K storage for 24 h in toluene (Fig. S17, ESI†), indicating that there is no racemization from the dissociation of the complex during the storage period. These interesting findings will promote the development of CPL-emissive functional materials by molecular engineering.

Conclusions

In summary, we demonstrated the first examples of rationally designed terthiophene-modified tetra-BF_2 complexes by Suzuki–Miyaura coupling reactions. The substituted position of the terthiophene group affected the photophysical properties to produce yellow-green and yellow emission colors with a sufficiently high quantum yield. The key factor is the π-conjugation extension and enhanced ICT interactions compared with the non-functionalized tetra-BF_2 complex. High g_{lum} (up to the order of 10^{-2}) and CPL brightness (125.2 M^{-1} cm^{-1}) were achieved by the tetra-BF_2 complex with terthiophene substituents on the *para*-position of the pyridine part in the molecular structures. Our study highlights the effect of balancing the electric and magnetic transition dipole moments to achieve a highly CPL-emissive performance, supported by the DFT calculations and experimental data. This work will enrich the molecular design of multinuclear boron complex engineering for novel CPL emitters as potential candidates for future applications in CPL-active systems.

Conflicts of interest

There are no conflicts to declare.

Acknowledgements

This work was supported by JSPS KAKENHI Grant Number JP21H05400. We thank the support from the Toyota Riken Scholar Program, the TOBE MAKI Scholarship Foundation, and the Nissan Chemical Corporation. This work was also supported by the Kyushu University Platform of Inter-/Transdisciplinary Energy Research (Q-PIT) through its "Module-Research Program". The computation was carried out using the computer resource offered under the category of general projects by Research Institute for Information Technology, Kyushu University.

Notes and references

1 J. Han, S. Guo, H. Lu, S. Liu, Q. Zhao and W. Huang, *Adv. Opt. Mater.*, 2018, **6**, 1800538.
2 Y. Gao, C. Ren, X. Lin and T. He, *Front. Chem.*, 2020, **8**, 458.
3 L. E. MacKenzie and R. Pal, *Nat. Rev. Chem.*, 2021, **5**, 109.
4 D. Parker, J. D. Fradgley and K.-L. Wong, *Chem. Soc. Rev.*, 2021, **50**, 8193.
5 Q. Cheng, A. Hao and P. Xing, *Nat. Commun.*, 2021, **12**, 6320.
6 J. Gong and X. Zhang, *Coord. Chem. Rev.*, 2022, **453**, 214329.
7 W.-L. Zhao, M. Li, H.-Y. Lu and C.-F. Chen, *Chem. Commun.*, 2019, **55**, 13793.
8 J.-K. Li, X.-Y. Chen, Y.-L. Guo, X.-C. Wang, A. C.-H. Sue, X.-Y. Cao and X.-Y. Wang, *J. Am. Chem. Soc.*, 2021, **143**, 17958.
9 H. Kubo, T. Hirose, T. Nakashima, T. Kawai, J.-Y. Hasegawa and K. Matsuda, *J. Phys. Chem. Lett.*, 2021, **12**, 686.
10 T. Mori, *Chem. Rev.*, 2021, **121**, 2373.
11 H. Kubo, T. Hirose, D. Shimizu and K. Matsuda, *Chem. Lett.*, 2021, **50**, 804.
12 K. Usui, N. Narita, R. Eto, S. Suzuki, A. Yokoo, K. Yamamoto, K. Igawa, N. Iizuka, Y. Mimura, T. Umeno, S. Matsumoto, M. Hasegawa, K. Tomooka, Y. Imai and S. Karasawa, *Chem. – Eur. J.*, 2022, e202202922.
13 Y. Tanaka, T. Murayama, A. Muranaka, E. Imai and M. Uchiyama, *Chem. – Eur. J.*, 2020, **26**, 1768.
14 T. Ono, K. Ishihama, A. Taema, T. Harada, K. Furusho, M. Hasegawa, Y. Nojima, M. Abe and Y. Hisaeda, *Angew. Chem., Int. Ed.*, 2021, **60**, 2614.
15 K. Ishihama, T. Ono, T. Okawara, T. Harada, K. Furusho, M. Hasegawa, Y. Nojima, T. Koide, M. Abe and Y. Hisaeda, *Bull. Chem. Soc. Jpn.*, 2021, **94**, 573.
16 K. Yao, Y. Li, Y. Shen, Y. Quan and Y. Cheng, *J. Mater. Chem. C*, 2021, **9**, 12590.

17 K. Takaishi, T. Matsumoto, M. Kawataka and T. Ema, *Angew. Chem., Int. Ed.*, 2021, **60**, 9968.
18 Y. Nojima, M. Hasegawa, N. Hara, Y. Imai and Y. Mazaki, *Chem. – Eur. J.*, 2021, **27**, 5923.
19 J. K. Cheng, S.-H. Xiang, S. Li, L. Ye and B. Tan, *Chem. Rev.*, 2021, **121**, 4805.
20 Y. Morisaki and Y. Chujo, *Bull. Chem. Soc. Jpn.*, 2019, **92**, 265.
21 K.-i Sugiura, *Front. Chem.*, 2020, **8**, 700.
22 A. Garci, S. Abid, A. H. G. David, M. D. Codesal, L. Đorđević, R. M. Young, H. Sai, L. L. Bras, A. Perrier, M. Ovalle, P. J. Brown, C. L. Stern, A. G. Campaña, S. I. Stupp, M. R. Wasielewski, V. Blanco and J. F. Stoddart, *Angew. Chem., Int. Ed.*, 2022, **61**, e202208679.
23 I. Roy, A. H. G. David, P. J. Das, D. J. Pe and J. F. Stoddart, *Chem. Soc. Rev.*, 2022, **51**, 55578.
24 S. Sato, A. Yoshii, S. Takahashi, S. Furumi, M. Takeuchi and H. Isobe, *Proc. Natl. Acad. Sci. U. S. A.*, 2017, **114**, 13097.
25 M. Hasegawa, Y. Nojima and Y. Mazaki, *ChemPhotoChem*, 2021, **5**, 10428.
26 J. Kumar, T. Nakashima and T. Kawai, *J. Phys. Chem. Lett.*, 2015, **6**, 3445.
27 Y. Sang, J. Han, T. Zhao, P. Duan and M. Liu, *Adv. Mater.*, 2020, **32**, 1900110.
28 F. Song, Z. Zhao, Z. Liu, J. W. Y. Lam and B. Z. Tang, *J. Mater. Chem. C*, 2020, **8**, 3284.
29 H. Zhang, J. Han, X. Jin and P. Duan, *Angew. Chem., Int. Ed.*, 2021, **60**, 4575.
30 P. Liao, S. Zang, T. Wu, H. Jin, W. Wang, J. Huang, B. Z. Tang and Y. Yan, *Nat. Commun.*, 2021, **12**, 5496.
31 S. Fa, T. Tomita, K. Wada, K. Yasuhara, S. Ohtani, K. Kato, M. Gon, K. Tanaka, T. Kakuta, T.-A. Yamagishi and T. Ogoshi, *Chem. Sci.*, 2022, **13**, 5846.
32 H. Tanaka, Y. Inoue and T. Mori, *ChemPhotoChem*, 2018, **2**, 386.
33 S. Wang, D. Hu, X. Guan, S. Cai, G. Shi, Z. Shuai, J. Zhang, Q. Peng and X. Wan, *Angew. Chem., Int. Ed.*, 2021, **60**, 21918.
34 Y. Qin, X. Liu, P.-P. Jia, L. Xu and H.-B. Yang, *Chem. Soc. Rev.*, 2020, **49**, 5678.
35 Z. Shi, X. Han, W. Hu, H. Bai, B. Peng, L. Ji, Q. Fan, L. Li and W. Huang, *Chem. Soc. Rev.*, 2020, **49**, 7533.
36 F.-Z. Li, J.-F. Yin and G.-C. Kuang, *Coord. Chem. Rev.*, 2021, **448**, 214157.
37 H. Lu, J. Mack, T. Nyokong, N. Kobayashi and Z. Shen, *Coord. Chem. Rev.*, 2016, **318**, 1.
38 E. M. Sánchez-Carnerero, F. Moreno, B. L. Maroto, A. R. Agarrabeitia, M. J. Ortiz, B. G. Vo, G. Muller and S. D. L. Moya, *J. Am. Chem. Soc.*, 2014, **136**, 3346.
39 I.-S. Tamgho, A. Hasheminasab, J. T. Engle, V. N. Nemykin and C. J. Ziegler, *J. Am. Chem. Soc.*, 2014, **136**, 5623.
40 S. Boodts, E. Fron, J. Hofkens and W. Dehaen, *Coord. Chem. Rev.*, 2018, **371**, 1.
41 A. N. Bismillah and I. Aprahamian, *Chem. Soc. Rev.*, 2021, **50**, 5631.
42 C. Yu, Z. Huang, X. Wang, W. Miao, Q. Wu, W.-Y. Wong, E. Hao, Y. Xiao and L. Jiao, *Org. Lett.*, 2018, **20**, 4462.
43 C. Yu, X. Fang, Q. Wu, L. Jiao, L. Sun, Z. Li, P.-K. So, W.-Y. Wong and E. Hao, *Org. Lett.*, 2020, **22**, 4588.
44 S. P. Parambil, F. d Jong, K. Veys, J. Huang, S. P. Veettil, D. Verhaeghe, L. V. Meervelt, D. Escudero, M. V. d Auweraer and W. Dehaen, *Chem. Commun.*, 2020, **56**, 5791.
45 M. Ihara, L. Cui, Y. Konishi, Y. Hisaeda and T. Ono, *Chem. Lett.*, 2022, **51**, 300.
46 L. Cui, H. Shinjo, T. Ichiki, K. Deyama, T. Harada, K. Ishibashi, T. Ehara, K. Miyata, K. Onda, Y. Hisaeda and T. Ono, *Angew. Chem., Int. Ed.*, 2022, **61**, e202204358.
47 Y. Liu, Z. Ma, Z. Wang and W. Jiang, *J. Am. Chem. Soc.*, 2022, **144**, 11397.
48 K. Dhbaibi, L. Abella, S. Meunier-Della-Gatta, T. Roisnel, N. Vanthuyne, B. Jamoussi, G. Pieters, B. Racine, E. Quesnel, J. Autschbach, J. Crassous and L. Favereau, *Chem. Sci.*, 2021, **12**, 5522.
49 L. Arrico, L. D. Bari and F. Zinna, *Chem. – Eur. J.*, 2021, **27**, 2920.